



Contents lists available at <http://qu.edu.iq>

Al-Qadisiyah Journal for Engineering Sciences

Journal homepage: <https://qjes.qu.edu.iq>



# Numerical investigation of the electric double-layer effect on the performance of microchannel heat exchanger at the combined electroosmotic and pressure-driven flow

*Dunya A. Mohammad\**, *Mushtaq I. Husan*, and *Ahmed J. Shkarah*

*Department of Mechanical Engineering, College of Engineering, University of Thi-Qar, Iraq*

## ARTICLE INFO

### Article history:

Received 4 January 2021

Received in revised form 8 February 2021

Accepted 29 March 2021

### Keywords:

Heat exchanger

Electric double layer

Electroosmotic flow

Pressure-driven

Numerically investigated

Poisson-Boltzmann

## ABSTRACT

Numerically investigated the electric double layer (EDL) Effects on the performance of the square microchannel heat exchanger (MCHE) at combined electro-osmotic and pressure-driven flow with compared pure pressure-driven with a hydraulic diameter (10 – 50)  $\mu\text{m}$ . We defined at any size (Dh) of microchannel heat exchanger become the impact of EDL is very slight with the studied effect of electric double layer thickness  $\lambda$ . The diluted water 1:1 potassium chloride (KCl) solution is used as a working fluid at an ionic concentration ( $10^{-4}$ ,  $10^{-6}$ ) M, silicon microchannel at zeta potential of surface -0.2 volt. A three-dimensional (3D) Poisson-Boltzmann equations and Navier-stokes equations with applied electric field are solved by using the finite volume scheme in this work. The results show an increase in pressure drop of the microchannel heat exchanger at combined flow electroosmotic and pressure-driven flow with a percentage of 31.09 % at an ionic concentration  $10^{-4}$  M and 42.71 % at  $10^{-6}$  M, increase in pumping power, especially at low ionic concentration. Slight enhancement in average heat transfer rate and effectiveness due to an increase in average temperature difference. Decrease in overall performance at combined electroosmotic and pressure-driven flow compared with pure pressure driven.

© 2021 University of Al-Qadisiyah. All rights reserved.

## 1. Introduction

In recent decades, rapid progress is observed in the manufacturing of microsystems (which have a length between 1  $\mu\text{m}$  – 1 mm), especially in micro-electronic mechanics system (MEMS) which integrates mechanical and electrical systems. The development in MEMS caused an augmentation in understanding the structure and flow of fluid. Manufacture of microelectronic mechanic's system (MEMS) by using different techniques such as bulk silicon micromachining, surface silicon micromachining, lithography, electro-discharge machining (EDM), and plastic modeling. Mushtaq I. Hasan et al. [1].

The basic phenomena of electro-kinetic in the microchannel can be classified into electro-osmosis, Electrophoresis, electro-migration, and Streaming potential. The process of transporting fluid in a microchannel subjected to an electric field is called electro-osmotic flow or pressure gradient is called pressure-driven flow or transport of fluid by an applied electric field and pressure-driven together this called combined electroosmotic and pressure-driven flow Berli [2]. A number of studies investigated the effect of EDL at pressure-driven or combined electroosmotic and pressure-driven flow.

\* Corresponding author.

E-mail address: [donia.ali@utq.edu.iq](mailto:donia.ali@utq.edu.iq) (Dunya Mohammad)



**Nomenclature**

$A$	Cross-section area ( $m^2$ )
$C_p$	Specific heat (J/kg.K)
$D_h$	Hydraulic diameter ( $\mu m$ )
$H$	Height ( $\mu m$ )
$K$	Thermal conductivity (J/k)
$L$	Length channel of heat exchanger ( $\mu m$ )
$M$	Mass flow rate (Kg/s)
$P$	Pressure (Pa)
$P.P$	Pumping power (watt)
$Q$	Heat transfer rate (watt)
$Re$	Reynold number
$T$	Temperature (K)
$t$	Separating wall thickness ( $\mu m$ )
$U$	Velocity in the x-direction (m/s)
$V$	Velocity in the y-direction (m/s)
$w$	Velocity in the z-direction (m/s)

*Greek symbols*

$\rho$	Density
$\mu$	Viscosity
$\zeta$	Zeta potential
$\psi$	Electric potential
$\kappa$	Debye-Huckel parameter
$\lambda$	EDL thickness
$\varepsilon$	Permittivity

*Subscripts*

EOF	Electro-osmotic flow
PDF	Pressure driven flow
EDL	Electric double layer
i	inlet
o	outlet
c	Cold fluid
h	Hot fluid

For instance, Chun and Li (1997) [3] numerically studied the impact of the electrical double layer (EDL) on the flow of liquid, pressure distribution, streaming potential, and friction coefficient for rectangular microchannels. 2D Poisson-Boltzmann equation and the exact solution to the motion equation were solved by recruiting the green function formulation. They found that high zeta potential and low value of ionic concentration lead to a great effect of electric double layer field on the flow of liquid. The increase in pressure drop caused increased induced electro-kinetic potential, while the increase in the ionic concentration of solution leads to a decrease in induced electro-kinetic. The EDL effect caused an increment in friction coefficient and viscosity apparent compared with no electric double layer effect. Prashanta D. and Ali B. (2001) [4] conducted an analytical solution of steady Newtonian flow through a 2D straight channel with combined pressure-driven flow PDF and electro-osmotic flow EOF at constant zeta potential of wall and constant buffer concentration. Pressure gradient, mass flow rate, and vorticity in combined PDF/EOF were investigated. The shear stress of the wall depended on three parameters (effective electric double layer thickness, EDL vorticity thickness, and EDL displacement thickness. Their results indicate to (1) the distribution of electro-osmotic potential  $\Psi^*$  is a relationship (function) of  $\alpha$  (the ionic energy parameter) only. (2) They defined an effective electric double-layer thickness as a function of  $\alpha$  (ionic energy parameter) and clarify that the EDL effects are confined to a region  $x \leq$  EDL thickness. (3) Defect in mass flow rate because of the distribution of velocity within EDL, this defect depended on EDL displacement. (4) For combined EOF/PDF, they explained that using Helmholtz velocity as an appropriate condition between the electric double layer is completed and bulk flow. Ng and Tan, (2006) [5], numerically investigated a single rectangular microchannel with an electrical double-layer (EDL) impact. Two models Poisson–Boltzmann model (PBM) and Nernst–Planck model (NPM) addition to Navier–Stokes equations were used to analyze the EDL effect in the channel. In comparison between the two models, it was found that the Poisson–Boltzmann model is better than the Nernst–Planck model in terms of cost (RAM and CPU). In addition, the P-B-M showed less contradiction of modeling the electric double layer a far about surface of the microchannel. They concluded that by reducing friction confidence at an increase in the Schmidt number ( $Sc$ ), the electric double layer (EDL) effects lead to an increase in the Schmidt number and hence the decrease in friction coefficient.

Thus, the Poisson–Boltzmann model(PBM) is still an attractive model to compute the electrical double layer (EDL) effect in the microchannel.

Dayong Y. (2011) [6] analytical solution of velocity distribution and potential for combined pressure-driven flow and electroosmotic flow in microchannel. The mathematical model to simulate fluid flow consisted of the Navier Stokes and the Poisson Boltzmann equations, which were solved by using the finite element method in Matlab software. Their results showed that at combined EOF/PDF the distribution of velocity is parabolic and compound of plug-like when the fluid is steady-state, the distribution of velocity is observed to be plug-like and similar to the EDL potential profile even in the case of pure EOF. Their results supply the guidelines for applications of combined flow (EOF/PDF) in microchannel chips. Nandy et al. (2013) [7] experimental study to improve the heat transfer performance by decreasing hydraulic diameter size or by using better thermal conductivity for working fluid in microchannel heat exchangers in addition to studying the testing and design of microchannel heat exchangers (MCHE). Working fluids are distilled water, water nanofluid (Al<sub>2</sub>O<sub>3</sub>) at volume concentrations 1%, 3%, and 5%, and water nanofluids (SnO<sub>2</sub>) at volume concentration 1%. They concluded to enhance the heat transfer rate by adding Nanoparticles in the fluid, water 50% (Al<sub>2</sub>O<sub>3</sub>) and water-nano fluids 1% (SnO<sub>2</sub>) greater absorption of the heat with 9% and 12% comparison with base fluid also higher overall heat transfer coefficient than the base fluid. Mushtaq et. al. (2017)[8] applied numerical investigation of two electrolyte solutions water and PBS (Phosphate- Buffered-saline solution) through the square microchannel by solving Navier stokes equation, Laplace and Poisson equation with the pure electro-osmotic flow. It was found that the water solution gives lower flow and velocity compared with PBS, and it was noticed a very small increase in temperature because of the simple effect of Joule heating. Moreover, it was concluded that zeta potential and electric field have a great effect on flow rate. Mushtaq et. al. (2017) [9] studied the pure electro-osmotic flow through a microchannel with contractions to contribute to an increase in the biomolecule flow corresponding to the used different shapes (rectangular, trapezoidal, curved, and triangular) of contractions. COSMOL software to analyze the flow behavior was used. Their results showed that the distribution of velocity for triangular contraction has higher values of flow velocity, and is highest compared to other geometries of contractions. In addition, it was concluded that the velocity of flow increased with the increase of zeta potential and electric field. Ahmed A. et al. (2019) [10] numerically investigated of scaling effect (surface roughness effects) of parallel flow in the square microchannel heat exchanger on thermal and hydrodynamic performance at various hydraulic diameters. It was concluded that the impact of surface roughness leads to improve thermal performance and an increase in pressure difference. The effect of roughness reduced with

increment  $Re$  and hydraulic diameter. Ahmed A. et al. (2019) [11] numerically studied of scaling effect (slip flow effects) in counter flow MCHE on performance at different geometries (square, trapezoidal, triangle, and circular). In addition, changing the size of a channel on thermal and hydrodynamic performance was studied. Their results indicated that the trapezoidal channel has higher overall performance compared to other shapes. Moreover, the triangle shape has a higher effect on slip flow and hence the square shape. It was found that greater slip flow is related to small velocity and hydraulic diameter. Thus, the slip flow causes an increase in pressure difference and pumping power. Qingkai et al. (2020) [12] theoretically investigated heat transfer and flow of a nanofluid in a horizontal microchannel in combination with the effect of an electric double layer and magnetic field. momentum equation with the presence of the EDL effect was solved. In addition, nanoparticle volume fraction, temperature, velocity, the Brinkman number ( $Br$ ), Hartmann number  $Ha$ , the impact of parameter  $k$ , and various physical quantities were discussed thoroughly. The finding indicates that the electric double layer and magnetic field may be used to control the heat transfer and flow in the microchannel. The heat improvement depends on the temperature applied on the wall and the Brinkman number. The magnetic field impact on friction coefficient and nanoparticle volume fraction can disregard the impact of the magnetic field on the Sherwood number and Nusselt number. Ahamed C. et al. (2020) [13] numerically studied electro-osmotic /pressure-driven flow with triangular obstacles (block) through rectangular microchannel by alternative technique CFD and modified IBM to solve Navier stokes equation with Poisson Boltzmann equation and Nernst Plank equation. They used a hybrid technique to improve the mixing efficiency of the Passive and active integration ways. Their findings refer to (a) The mixing efficiency depended on a change in several triangular blocks, the zeta potential of surface, and EDL thickness (b) the Mixing efficiency reduced with an increase in an applied electric field, Reynold number, and Peclet number. (c) Mixing efficiency is higher from 28.2 – 50.2 % at increments in the number of a block from (1- 5).

## 2. Problem description:

In this paper, a three-dimension parallel flow square microchannel heat exchanger (MCHE) as shown in Fig. 1 is modeled. study one unit of microchannel heat exchanger consists of hot and cold fluid as shown in Fig. 2. The length of the heat exchanger is  $L=1\text{mm}$  and its hydraulic diameter (is  $10\text{-}50\mu\text{m}$ ). The thickness of the wall between the hot channel and cold channel is equal to  $t=3\mu\text{m}$ , while the ratio between the velocity of pressure-driven to the velocity of electro-osmotic flow is 0.96. the temperature of the inlet hot and cold are 373 k, 293 k receptivity. The zeta potential of the channel surface (-0.2 volt), and the applied field electric  $E_z$  on working fluid ( $10^6$  volt/m. The electric double layer overlaps the effect on mixing efficiency. Their findings are useful in a lot of fields (Biomedical, cooling of microchips, deoxyribonucleic acid hybridization, and biotechnological. Most of the previous papers theoretical and practical investigated heat transfer and flow characteristics in a single microchannel. This study investigates the effect of an electric double layer (EDL) at two values of ionic concentration through a parallel flow microchannel heat exchanger (PMCHE) and determines at any size of the microchannel heat exchanger stops the EDL effect or if the slight effect. Compared the results with no electric double layer (EDL) effect (pure pressure-driven).

## 2.1. Electric Double Layer (EDL)

The electrical potential surface for a solid wall of the microchannel and the liquid has quantities of ions, this leads to the attraction of the counterions in dilute liquid to electrostatic charges of the surface to create an electric field. The order of electrostatic charge and ions of liquid is called electric double layer (EDL) as shown in Fig. 3. There are two types of ions in terms of motion, for the compact layer (the layer near of surface) the ions are immobile, and in the diffuse double layer (DDL) the electric field less influence on the ions (mobile). At the dilute liquid flow through the microchannel, the mobile ions of the electric double layer create an electric current (streaming current) to flow with liquid flow. In case the streaming potential of electro-osmotic is very small compared to the applied external electric field. The gathering of the ions in the direction of flow sets up an electric potential and electric field together known as streaming potential, this caused in creates a current called conduction current. The conduction current direction is counter to the direction of liquid flow. The maximum value of the thickness of the electric double layer (EDL)  $1\mu\text{m}$  depending on the properties of the liquid are (a) ionic concentration (b) temperature of the dilute liquid, and (c) zeta potential of the surface. To show characterize of the electric double layer (EDL) effects used the Debye-Huckel parameter  $k$  [13], which represented the thickness of the electric double layer (EDL) Kumar [15].

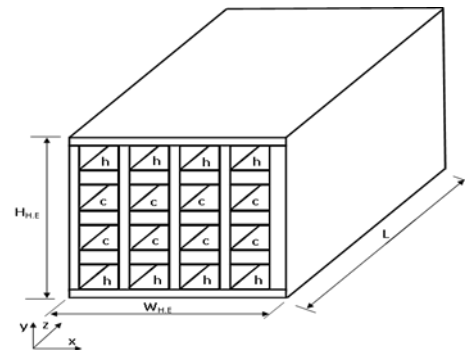


Figure 1. Schematic model of microchannel heat exchanger

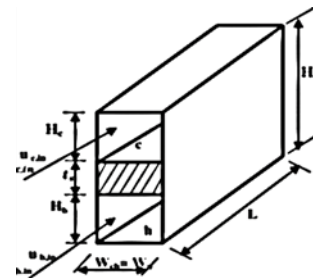
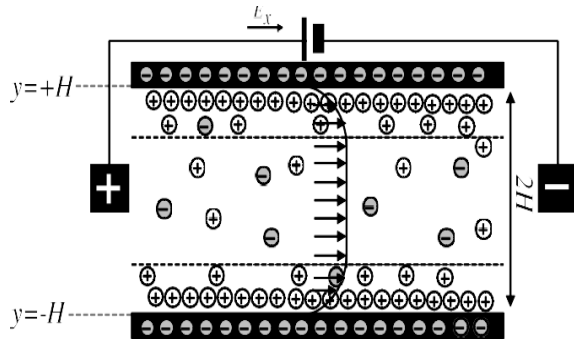


Figure 2. A unit of heat exchange consists of hot and cold channels [14].



**Figure 3.** Scheme formed of an electric double layer on the surface wall [16]

### 3. Mathematical formulation

Governing Equations 3D steady-state, incompressible, and laminar flow, the following equations are solved to calculate the distributions of velocity, temperature, and EDL distribution for parallel flow microchannel heat exchanger.

#### Poisson's equation:

According to the theory of electrostatics, the relationship between  $\Psi$  and  $\rho_e$  is given by Poisson's equation Sheikhizad et al. [17], which is for a rectangular channel.

$$\frac{\partial^2 \Psi}{\partial x^2} + \frac{\partial^2 \Psi}{\partial y^2} + \frac{\partial^2 \Psi}{\partial z^2} = -\frac{\rho_e}{\epsilon \epsilon_0} \quad (1)$$

$\epsilon$  is the dielectric constant of the medium

$\epsilon_0$  is the electric permittivity of a vacuum.

$\rho_e$  is the net volume charge density, we have?

$$n_i = n_{oi} \exp\left(-\frac{z_i e \Psi}{k_b T}\right) \quad (2)$$

$$\rho_e = (n^+ - n^-) = -2n_o z e \sinh\left(\frac{z e \Psi}{k_b T}\right) \quad (3)$$

$n^+$  and  $n^-$  are a concentration of cations and anions, respectively.

$k_b$  Boltzmann's constant =  $1.3805 \times 10^{-23} \text{ J mol}^{-1} \text{ K}^{-1}$ .

$e$  electron charge =  $1.6021 \times 10^{-19} \text{ C}$ .

$n_{oi}$  bulk concentration. So, Poisson-Boltzmann Eq. (1) become :

$$\frac{\partial^2 \Psi}{\partial x^2} + \frac{\partial^2 \Psi}{\partial y^2} + \frac{\partial^2 \Psi}{\partial z^2} = \frac{2n_o z e}{\epsilon \epsilon_0} \sinh\left(\frac{z e \Psi}{k_b T}\right)$$

**Continuity equation [5]:**

$$\frac{\partial u}{\partial x} + \frac{\partial v}{\partial y} + \frac{\partial w}{\partial z} = 0 \quad (4)$$

**Momentum equation:**

x-direction

$$u \frac{\partial u}{\partial x} + v \frac{\partial v}{\partial y} + w \frac{\partial w}{\partial z} = \frac{\mu}{\rho} \left( \frac{\partial^2 u}{\partial x^2} + \frac{\partial^2 u}{\partial y^2} + \frac{\partial^2 u}{\partial z^2} \right) - \frac{\mu}{\rho} \frac{\partial p}{\partial x} \quad (5)$$

y- direction

$$u \frac{\partial v}{\partial x} + v \frac{\partial v}{\partial y} + w \frac{\partial v}{\partial z} = \frac{\mu}{\rho} \left( \frac{\partial^2 v}{\partial x^2} + \frac{\partial^2 v}{\partial y^2} + \frac{\partial^2 v}{\partial z^2} \right) - \frac{\mu}{\rho} \frac{\partial p}{\partial y} \quad (6)$$

The applied electric field ( $Ez \rho_e$ )

$$u \frac{\partial w}{\partial x} + v \frac{\partial w}{\partial y} + w \frac{\partial w}{\partial z} = \frac{\mu}{\rho} \left( \frac{\partial^2 w}{\partial x^2} + \frac{\partial^2 w}{\partial y^2} + \frac{\partial^2 w}{\partial z^2} \right) - \frac{1}{\rho} \frac{\partial p}{\partial z} - Ez \rho_e \quad (7)$$

Energy equation:

$$u \frac{\partial T}{\partial x} + v \frac{\partial T}{\partial y} + w \frac{\partial T}{\partial z} = \frac{k}{\rho C_p} \left( \frac{\partial^2 T}{\partial x^2} + \frac{\partial^2 T}{\partial y^2} + \frac{\partial^2 T}{\partial z^2} \right) \quad (8)$$

The heat transfer rate of a microchannel heat exchanger between hot and cold [1]:

$$Q = m C_p \Delta T \quad (9)$$

$$\text{The effectiveness } (\epsilon) = \frac{Q_{\text{act}}}{Q_{\text{max}}} = \frac{C_h (T_{hi} - T_{ho})}{C_{\text{min}} (T_{hi} - T_{ci})} = \frac{C_c (T_{co} - T_{ci})}{C_{\text{min}} (T_{hi} - T_{ci})} \quad (10)$$

The overall performance of MCHE can be calculated from eq. (11)

$$\eta = \frac{\epsilon}{\Delta P t} \quad (11)$$

$$\Delta P t = \Delta P C + \Delta P h = (P_{in, C} - P_{O, C}) + (P_{in, h} - P_{O, h}) \quad (12)$$

**The boundary conditions [17]**

At the inlet of the channel  $Z = 0$ , then

$$U = 0$$

$$V = 0$$

$$W = U_{in} \text{ \& } T = T_{in}.$$

At the outlet of the channel  $Z = LCh$  and the flow is fully developed, then

$$\frac{\partial u}{\partial z} = 0$$

$$\frac{\partial v}{\partial z} = 0$$

$$\frac{\partial w}{\partial z} = 0 \text{ \& } \frac{\partial T}{\partial z} = 0$$

For three cold walls adiabatic (sides walls and up the wall) and three hot walls adiabatic (sides walls and down the wall) conditions are applied:

$$u = 0 \quad v = 0 \quad w = 0 \quad \frac{\partial T}{\partial z} = 0$$

$$\text{At } x=0, \quad \Psi = \zeta_0$$

$$x=w, \quad \Psi = \zeta_0$$

$$\text{At } y=0, \quad \Psi = \zeta_0$$

$$\text{At } y=h, \quad \Psi = \zeta_0$$

For the up wall of the hot channel and down wall of the cold channel:

$$\Psi = \zeta_0$$

#### 4. Properties of material

Water is a working fluid with an aqueous KCL solution at the ionic concentration ( $10^{-4}$ M,  $10^{-6}$  M), vacuum permittivity (F/m)  $8.85 * 10^{-12}$ , dielectric constant  $\epsilon$  80 and  $6.39 * 10^{-10}$  The permittivity of water (C/V\*m). The data of the fluid (water) input by creating a User Defined Function (UDF).

**Table 1.** Shows the properties of dilute liquid and silicon.

material	Density (Kg/m <sup>3</sup> )	Cp (J/Kg.K)	K (W/m.K)	$\mu$ (Kg/m.s)
Dilute liquid	997	4182	0.605	0.9e-03
Silicon	2329	700	148	-

#### 5. Numerical solution

The system of governing equations and the Poisson-Boltzmann equation and boundary conditions are numerically solved using the finite volume method (FVM). A SIMPLE algorithm is used to solve the problem of velocity-pressure distribution and UDF to solve the Poisson-Boltzmann equation to study the effect electric double layer (EDL). Fluent19 software has been used to do the numerical solution.

Table 2 shows the independent grid size for hydraulic diameter (20 $\mu$ m) and its effect on the solution results.

**Table 2.** Mesh independent

Mesh size	Outlet temperature (K) of hot channel	Outlet temperature (K) of cold channel
Mesh 1 (size element =5 $\mu$ m)	318.253	347.748
Mesh 2 (size element =3 $\mu$ m)	318.287	347.573
Mesh 3 (size element =1 $\mu$ m)	318.204	347.302
Mesh 4 (size element = 0.8 $\mu$ m)	318.201	347.30

#### 6. Results and discussions

Numerical simulations of heat transfer and fluid flow problem were executed by using the commercial computational fluid dynamic (CFD) package. The governing equations for liquid flow were solved by finite volume method (FVM), and the SIMPLE algorithm has been used to solve the problem of velocity-pressure coupling. User-Defined Function (UDF) has been employed to solve the Poisson-Boltzmann equation to study the combination EOF/PDE flow through MCHE. The thickness of the electric double layer plays a significant role in combined electro-osmotic / pressure-driven flow due to its effect on the flow, temperature difference, and total pressure drop. The thickness of the electric double layer can be estimated from the Debye Huckel parameter  $\kappa$ , such refer  $1/\kappa$  to EDL thickness  $\lambda$ . The relation between EDL thickness and ionic concentration M is reversed and the increase in the ionic concentration of the solution leads to a decrease in EDL thickness ( $\lambda$ ). The parameters will be used in the investigation shown in Table 3. The parameter used in this paper is shown in Table 4.

**Table 3.** The parameters used in this paper.

The name	Value
the dielectric constant of the fluid	80
permittivity of vacuum	$8.85 * 10^{-12}$ C/V*m
The permittivity of fluid (water)	$6.93 * 10^{-10}$ C/V*m
Electric field	$10^6$ volt/m
Zeta potential	-200 mV
Ionic concentration	$10^{-4}$ & $10^{-6}$ M
Charge of electron	$-1.602 * 10^{-19}$ C
Valence (z)	1
Thickness of EDL	32 nm, 324 nm

Table 4 shows the percentage change (pure PDF and combined PDF /EOF) for square MCHE of the various parameters with the hydraulic diameter at two values of concentration. The percentage change of pressure drop is calculated from the following equation:

$$\text{The percentage change} = \frac{(\Delta P_{EOF\&PDF} - \Delta P_{PDF})}{\Delta P_{EOF\&PDF}}$$

The other parameter was calculated with the same method.

**Table 4.** Average percentage change of parameters

parameters	The percentage change % at $c=10^{-4}$	The percentage change % at $c=10^{-6}$
Total pressure drop	31.09	42.71
effectiveness	19.26	35.11
Overall performance	20.46	6.97

To validate the work of user-defined function (UDF) that was used to solve the Poisson Boltzmann equation and applied electric field compared the present model with pure electro-osmotic in microchannel [8]. The model presented in [8] is a microchannel that has a hydraulic diameter of 100  $\mu$ m, a width of channel of 100  $\mu$ m, a height of microchannel of 100  $\mu$ m, and a length of 500  $\mu$ m. They used a glass microchannel with zeta potential -0.1 volt and the water as a working fluid with ionic concentration  $3.727 * 10^{-6}$  M and applied electric field 100000 volt/m. The agreement between the present model and that for [8] is very good,

and the percentage of the error is 2 %. Fig. 4 shows the comparison between the results of the data of [8] for the velocity of electro-osmotic with a width of the microchannel and the result of the present model. To check the numerical model validity, verification was made by solving the model presented in [18] a compared the results. The model presented in [18] is a square microchannel at combined flow (electro-osmosis flow and pressure-driven flow) with a hydraulic diameter of 25  $\mu\text{m}$ , channel height of 25  $\mu\text{m}$ , a channel width of 25  $\mu\text{m}$ , and length of 100  $\mu\text{m}$  with  $\Delta P/dx = 10^5$  pa/m, an inlet temperature of 289 K, and a molar concentration  $10^{-4}\text{M}$ ,  $10^{-5}\text{M}$ , zeta potential  $\zeta = 150, 200$  mV. Fig. 5 shows the comparison between the results of the data of [18] for velocity distribution with a width of microchannel at different ionic concentrations. It can be seen that from this Fig. 5, there is a good agreement between the results of the present model and that for [18] and the error between the model presented and a result of [18] less than 5 %.

To show the distribution of velocity, pressure, and temperature using contours on created planes with the length and width of the microchannel heat exchanger.

Fig.6 explains the velocity distribution along the microchannel of the PFMCHHE (y-z) plane at the small size of channel  $D_h=10\ \mu\text{m}$  due to the ratio of EDL thickness to channel height is larger especially when higher zeta potential (-200 volt) and low ionic concentration. It can be noticed from this figure that the flow velocity in a center is maximum and minimum toward the wall as a result of the friction and the EDL field is opposite of the flow direction, this causes a disabled flow.

Fig. 7 represents the distribution of flow velocity for many planes (x-y) along hot and cold channels of parallel flow MCHE when  $D_h=10\ \mu\text{m}$  and  $Re=50$ . From Fig. 6 it is observed that the velocity at the center of the channel is higher and decreasing toward walls due to friction effects and the EDL field. Maximum velocity at the inlet flow and minimum value of the velocity at the outlet channel is observed due to losses. Fig. 8 shows the (z-y) plane for the pressure drop distribution contour at the same value of hydraulic diameter and  $Re$  along cold and hot channels of PFMCHHE. It can be concluded from the figure that, the pressure drop reduced with the flow as a result of losses due to friction and dynamic friction.

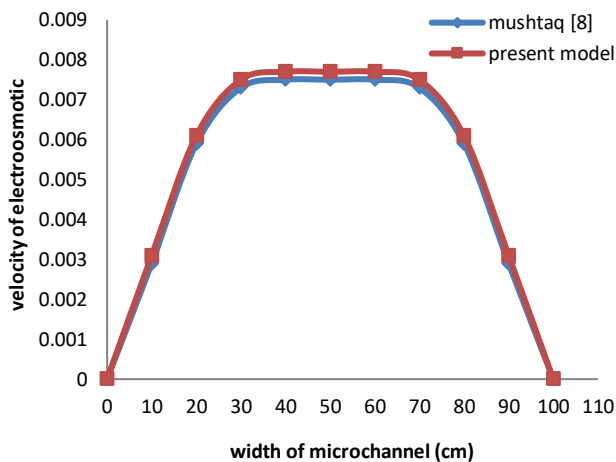


Figure 4. For the present model and that for [8].

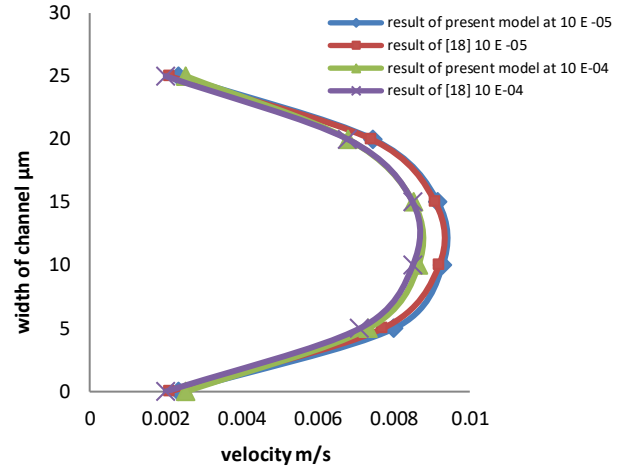


Figure 5. For the present model and that for [18].

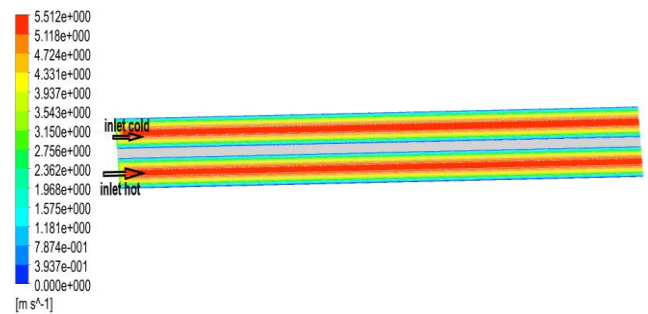


Figure 6. Contour explains the distribution of velocity (m/sec) at PFMCHHE on the (y-z) plane at  $D_h=10\ \mu\text{m}$  and  $Re=30$ .

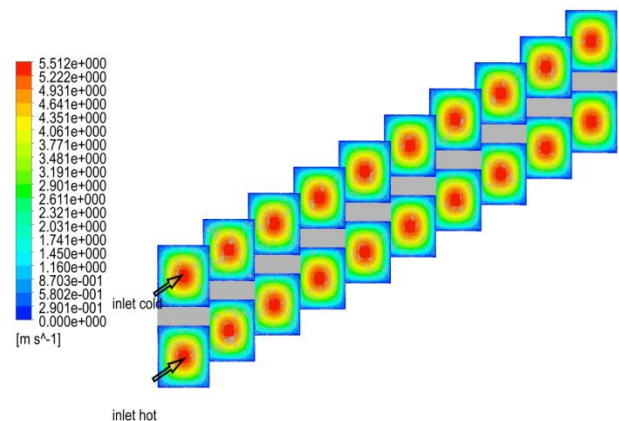
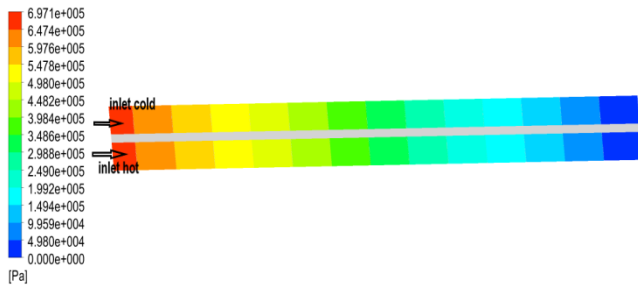


Figure 7. Contour represents the variation of velocity (m/s) along the hot and cold channels at parallel flow MCHE,  $D_h=10\ \mu\text{m}$ , and  $Re=30$ .



**Figure 8.** Contour pressure distribution along the cold channel and hot channel of parallel flow MCHE for  $D_h=10 \mu\text{m}$  and  $Re=30$ .

Fig. 9 displays the distribution of temperature contours along the length of the channel with a parallel flow microchannel heat exchanger. The inlet fluid of hot channel 373 K, and inlet fluid of cold channel 293 K at hydraulic diameter  $10 \mu\text{m}$ . It can be seen from Fig. 9 that, there is an increment in heat transfer and temperature difference with the dilute liquid flow, and reach a high value in the channel end due to heat exchange from the hot liquid to the cold liquid.

Fig. 10 explains the variation in the total pressure difference ( $\Delta P_t$ ) with hydraulic diameter for unit parallel microchannel heat exchanger at two cases of driven flow (electro-osmotic/pure pressure-driven flow) with two values of ionic concentration ( $10^{-6}$ ,  $10^{-4}$ ) M. From this figure, it can be observed that the total pressure drop declined with the increase of hydraulic diameter for two cases as a result of an increment in the cross-sectional area of an MCHE. In addition, it can be shown that higher pressure drop at combined EOF/PDF comparison with pure pressure-driven due to increase in velocity of liquid flow which caused larger losses in pressure.

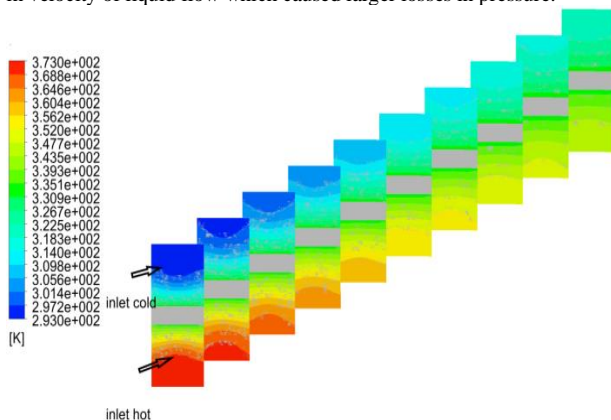
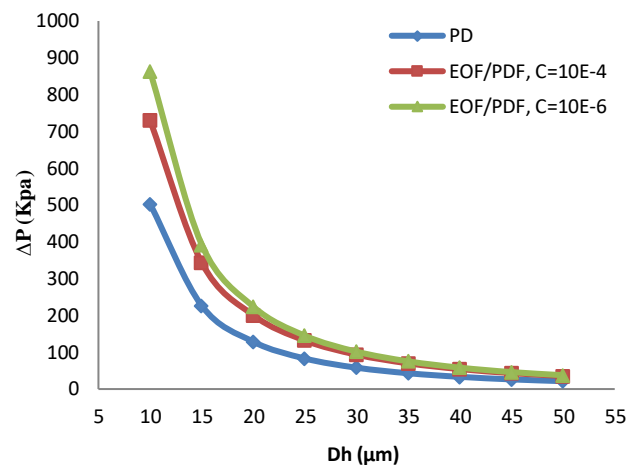


**Figure 9.** The contour of temperature distribution (K) for many planes of parallel flow MCHE  $D_h=10 \mu\text{m}$  and  $Re=50$ .

A low concentration leads to a higher pressure drop due to an increase in EDL thickness at low concentration can be seen from Fig. 10 that a low concentration leads to a higher pressure drop due to an increase in EDL thickness at low concentration, with notice that the impact of EDL lower

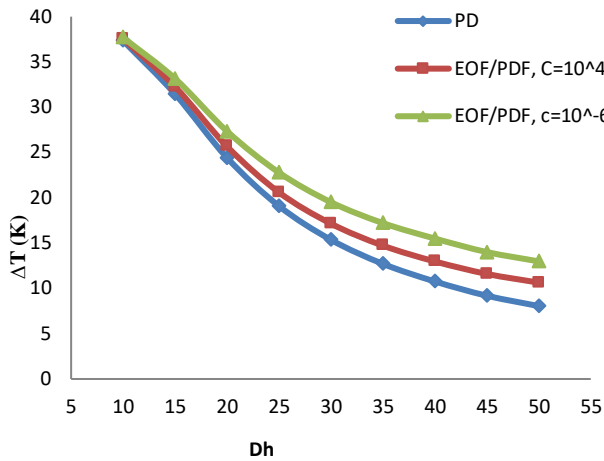
with increasing in hydraulic diameter depended on the ratio between the thickness of EDL to the height of the channel, at  $D_h > 40 \mu\text{m}$  begin the effect of EDL stop due to the large height of microchannel compared with the thickness of EDL. Fig. 11 shows the temperature difference variation ( $\Delta T$ ) for pure PDF and combined flow with a hydraulic diameter at two values of ionic concentrations (two values of EDL thickness). From the figure, it can be concluded that the temperature difference decrement with increasing hydraulic diameter for all cases. Can be noticed from Fig. 11 that, an increase in average temperature difference at combined flow compared with PDF especially at higher EDL thickness as a result of the flow of the electric double layer field in the opposite direction to the flow in the channel center, this lead to obstructing inflow at the surface of a channel at combined flow (EOF/PDF). The relation between the effectiveness ( $\epsilon$ ) and hydraulic diameter is shown in Fig. 12. It can be observed that the effectiveness is decreased with the increase of hydraulic diameter due to a decrease in temperature difference with the increased size of the channel. Moreover, the effectiveness in the case of combined flow is higher than that for pure PDF and the effectiveness increased with decreasing the concentration. The increase in effectiveness in the presence of EDL is due to an increase in temperature difference when mixed with EOF/PDF and the slight effect on effectiveness.

Fig. 13 represents the variation in the performance index ( $\eta$ ) with a size of a microchannel. It can be seen the performance index increased with increasing hydraulic diameter for all cases due to the decrease in total pressure with increased channel size. Furthermore, the impact of electric double-layer thickness has a significant impact on overall performance, which leads to a decrease in the performance index due to the increase in total pressure difference at combined driving. The performance index is observed to be decreased in the small size of the microchannel compared with pure pressure-driven and improvement in performance at large size of microchannel heat exchanger because of lower the ratio between the thickness of EDL to the height of the microchannel.



**Figure 10.** Variation of total pressure drop (KPa) with a hydraulic diameter ( $\mu\text{m}$ ).





**Figure 11.** Variation of average temperature difference with the hydraulic diameter ( $\mu\text{m}$ ).

The relationship between an average heat transfer rate ( $Q_{avg}$ ), hydraulic diameter for unit microchannel heat exchanger for two cases of pure pressure-driven and mixed-driven flow is shown in Fig. 14. It can be concluded that the heat transfer rate is increased with the increasing of hydraulic diameter for all cases as a result of an increment in the cross-sectional area of an MCHE. In this figure, the average heat transfer due to the lost heat is not equal to the heat gain of a combined PDF/EOF due to the formation of the EDL, which means an increase in the thickness of the separator wall. Fig. 14 shows an Enhancement in the average heat transfer rate in combined PDF/EOF at higher EDL thickness (low ionic concentration) due to an increase in the lost heat of the hot channel. Fig. 15 shows the variation in the pumping power (P.P) with hydraulic diameter. In addition, it can be observed that the relation of pumping power with channel size is steady as a horizontal line for all cases. This means the change in hydraulic diameter has no impact on pumping power. Can be seen from Fig. 15 that an increase in the pumping power at combined flow is due to an increase in total pressure drop and flow rate of liquid and higher pumping power at low ionic concentration.

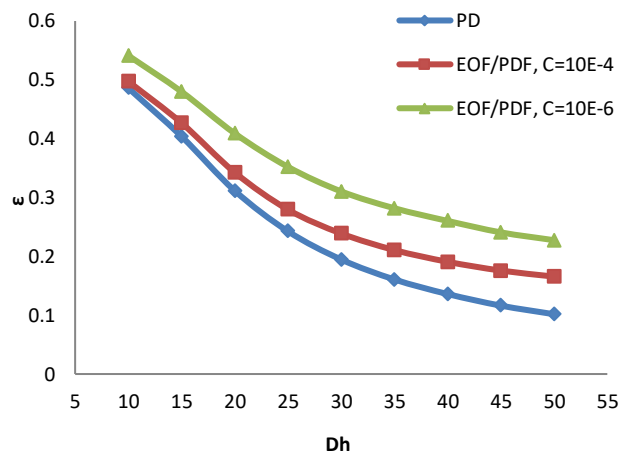


**Figure 12.** Variation of effectiveness with a hydraulic diameter ( $\mu\text{m}$ ).

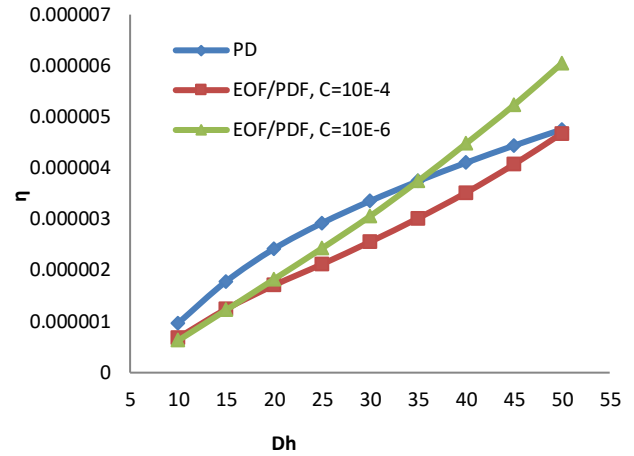


**Figure 13.** Variation of overall performance with a hydraulic diameter ( $\mu\text{m}$ ).

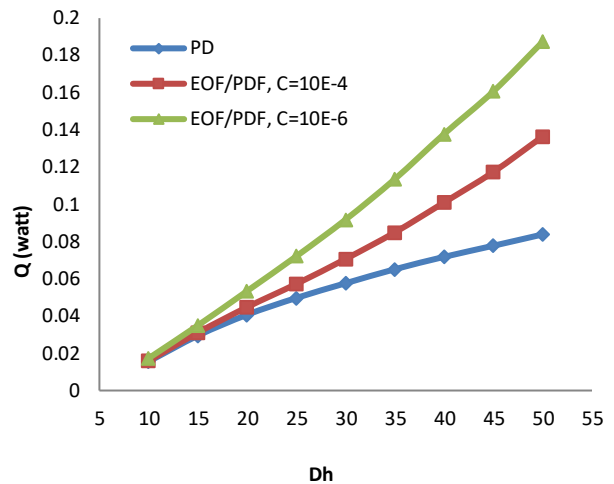


**Figure 14.** Variation of average heat transfer (watt) with a hydraulic diameter

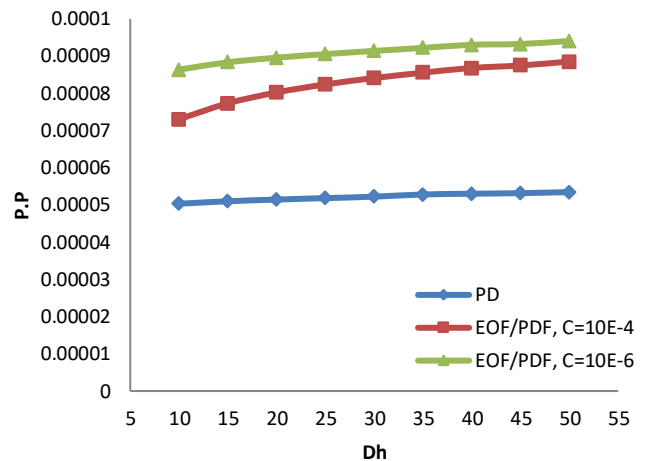


**Figure 15.** Variation of pumping power (watt) with a hydraulic diameter.



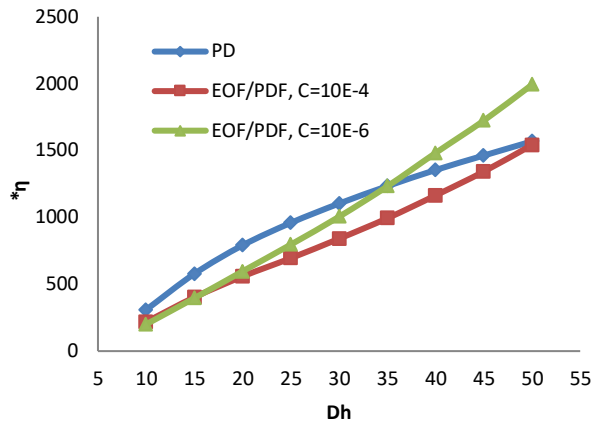


**Figure 16.** Variation of overall performance with a hydraulic diameter

Fig. 16 expresses the variation of the performance factor ( $\eta^*$ ) with hydraulic diameter. It can be seen from this figure that the performance factor increment with increasing hydraulic diameter due to an increase in the area of the microchannel. Moreover, it shows an increase in the heat exchanged with remaining pumping power at a constant value with changed channel size. For mixed PDF/EOF flow, it can be seen that the relationship between performance factor and size of the microchannel is linear, also notice that reduced performance factor, especially when the small size of the microchannel due to the higher effect of EDL with enhancement in performance factor at a large hydraulic diameter and low concentration.

Fig. 17 explains the variation of a temperature difference as a comparison between hot and cold channels with a hydraulic diameter at two values of ionic concentration. From the figure, it can be noticed that pressure-driven flow and temperature difference are similar for the two-channel (hot and cold). However, the temperature difference for a hot channel is higher than a cold channel especially for low ionic concentration depending on EDL thickness. The reason is attributed to the electric double layer thickness of an increase with an increase in temperature inlet of liquid.

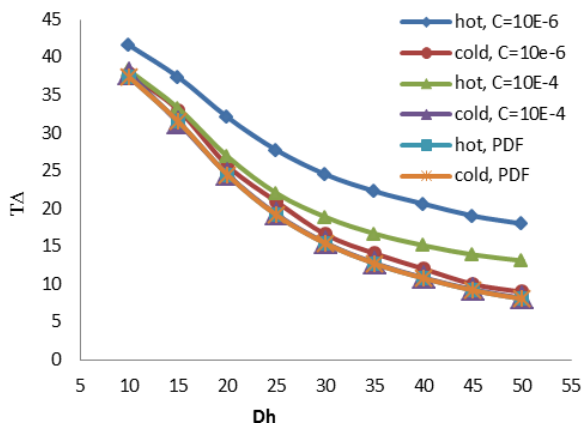


**Figure 17.** Variation of temperature is different for hot and cold channels with a hydraulic diameter ( $\mu\text{m}$ ).

The consequence leads to making the loss of heat not equal to the heat gain in the case of the presence of the electric double layer depending on ionic concentration and temperature inlet of liquid.

## 7. Conclusions

A numerical solution to study the effect of the electrical double layer (EDL) on the thermal and hydraulic performance of parallel flow microchannel heat exchangers by solving 3D Navier-stokes and 3D Poisson-Boltzmann equations was conducted. The results can be concluded that:

1. Increasing in total pressure drop at combined flow (electro-osmotic and pressure-driven flow) for parallel flow microchannel heat exchanger especially at a higher thickness of the electric double layer (low ionic concentration and higher zeta potential).
2. Notice the effects of EDL are very slight at the large size of hydraulic diameter  $D_h > 40 \mu\text{m}$  depending on the ratio of the thickness of the electric double layer to the height of the microchannel.
3. Enhancement in average heat transfer rate and effectiveness.
4. Higher pumping power at combined driven flow.
5. The thickness of the electric double layer has an important role in the effect of the flow rate and performance of the microchannel heat exchanger.
6. For pure pressure driven, the temperature difference for the hot channel is equal to the temperature difference for the cold channel (the heat gain is equal to heat loss).
7. For combined flow (PDF/EOF), the temperature difference for the hot channel is higher than for the cold channel.

## Authors' contribution

All authors contributed equally to the preparation of this article.

## Declaration of competing interest

The authors declare no conflicts of interest.

## Funding source

This study didn't receive any specific funds.

## REFERENCES

- [1] Mushtaq I. Hasan, A. Rageb, M. Yaghoubi, and Homayon Homayoni, Influence of channel geometry on the performance of a counter flow microchannel heat exchanger, *International Journal of Thermal Sciences*, 48 (2009) 1607–1618
- [2] Claudio Berli, Theoretical modeling of electrokinetic flow in microchannel networks, *Colloids and Surfaces A: Physicochemical. Eng. Aspects* 301 (2007) 271–280.
- [3] Chun Yang and Dongqing Li, Electrokinetic effects on the liquid flow in rectangular microchannels, *Journal of Colloid and Interface Science*, 149 (1997) 95–107.
- [4] Prashanta Dutta and Ali Beskok, Analytical Solution of Combined Electroosmotic/ Pressure Driven Flows in Two-Dimensional Straight Channels: Finite Debye Layer Effects, *Analytical Chemistry J.*, 73 (2001) 1979–1986.
- [5] Ng and Tan, Numerical analysis of EDL effect on heat transfer characteristic of 3-D developing flow in a microchannel, *Numerical Heat Transfer, Part A*, 49 (2006) 991–1007.
- [6] Dayong Yang, Analytical solution of mixed electroosmotic and pressure-driven flow in rectangular microchannels, *Key Engineering Materials*, 483 (2011) 679–

- 683.
- [7] Nandy Putra<sup>1</sup>, Wayan Nata Septiadi, Gerry Julian, Ary Maulana and Ridho Irwansyah, An experimental study on the thermal performance of Nanofluids in the microchannel heat exchanger, *International Journal of Technology*, 2 (2013) 167 - 177.
- [8] Mushtaq I. Hasan, Alaa M. Lafta, Ahmed J. Shkarah, Numerical investigation of electroosmotic flow in a microchannel, *International Review of Mechanical Engineering (I.R.M.E)*, 11(8) (2017).
- [9] Mushtaq I. Hasan, Alaa M. Lafta, Ahmed J. Shkarah, Study the electroosmosis flow in a microchannel with contractions of different geometries, *proc. Of the 2nd Int. sci. conf.*, Southern Technical University, (march 2017).
- [10] Ahmed A. Ali, Mushtaq I. Hassan, and Ghassan Adnan, Study surface roughness on the overall performance of parallel flow microchannel heat exchanger, the *University of Thi-Qar Journal for Engineering Sciences*, 10 (1), 2019.
- [11] Ahmed A. Ali, Mushtaq I. Hassan, and Ghassan Adnan, Numerical investigation of the slip flow effect in the counter-flow microchannel heat exchanger with different channels geometries, *First International scientific conference of Al-Ayen University (ISCAU)*, 2019.
- [12] Qingkai Zhao, Hang Xu, and Longbin Tao, Flow and heat transfer of nanofluid through a horizontal microchannel with magnetic field and interfacial electrokinetic effects, *European Journal of Mechanics/B Fluids*, 80 (2020) 72-79.
- [13] Ahamed Saleel, Asif Afzal, Mostafa Abdel Mohamed, Manzoor Elahi, H. Fayaz, Numerical investigation on pressure-driven electroosmotic flow and mixing in a constricted microchannel by a triangular obstacle, *International Journal of Numerical Methods for Heat & Fluid Flow*, (9 June 2020).
- [14] Mushtaq I. Hasan, Effect of variable fluid properties on the hydrodynamic and thermal characteristics of parallel flow microchannel heat exchanger, *Journal of University of Thi-Qar*, 10 (4), Dec. (2015).
- [15] S. Kumar, The EDL Effect in Microchannel Flow: A Critical Review, *International Journal of Advanced Computer Research*, 3 (4), (2013).
- [16] Ferrás, A. Afonso, M. Alves, J. Nóbrega and F. Pinho, Electro-osmotic and pressure-driven flow of viscoelastic fluids in microchannels: Analytical and semi-analytical solutions, *PHYSICS OF FLUIDS* 28 (2016) 093102
- [17] Mehdi Sheikhezad and Mohammad Kalteh, Heat transfer investigation of combined electroosmotic/pressure driven nanofluid flow in a microchannel: Effect of heterogeneous surface potential and slip boundary condition, *Journal Pre-proof*, (2019).
- [18] Reza Monazami and Mehrdad T. Manzari, Analysis of combined pressure-driven electroosmotic flow through square microchannels, *Microfluid Nanofluid*, 3 (2007) 123–126.